Zero- and Low-Bias Control Designs for Active Magnetic Bearings

Panagiotis Tsiotras, *Senior Member, IEEE,* and Brian C. Wilson

***Abstract*— In this paper we present several nonlinear control designs for a single one-degree-of-freedom (1-DOF) Active Magnetic Bearing (AMB). The primary control objective is to globally asymptotically stabilize the mechanical states of an AMB while reducing the AMB power losses. This suggests operation with zero or low bias flux. We derive a flux-based model for an AMB using a generalized complementary flux condition. This condition is imposed both for zero and low bias operations. A convenient model structure results, in which the zero-bias mode is a special case of the more general low-bias mode of operation. We next derive control laws for low- and zero-bias AMB operation. The control designs borrow ideas from the theory of control Lyapunov functions (clf's) and passivity. The performance of each proposed control design is evaluated via numerical simulations with a high-fidelity AMB model. Implementation issues are also discussed.**

***Index Terms*— Magnetic bearings, bias flux, passivity, nonlinear systems.**

I. Introduction

ACTIVE magnetic bearings (AMBs) have several advantages over conventional ball bearings. Their main advantage is frictionless operation due to lack of contact between the rotor and the stator. Maintenance of AMBs is also reduced due to lack of lubrication. Moreover, their potential to provide high-speed, frictionless operation and active disturbance rejection makes AMBs ideal candidates for several industrial applications such as, vacuum pumps, hard disk drives, high-speed centrifuges, high-speed flywheels, turbomachinery, etc.

Most importantly, active magnetic bearings are indispensable for the recently proposed high-speed electromechanical flywheel batteries. These devices have been advocated as an alternative to replace on-board chemical batteries for orbiting satellites, as well as for terrestrial applications [1], [2], [3]. To be competitive with other energy storage methods they need to operate at very high-speeds (at the order of 60-80K rpm). A primary concern for efficient operation of such energy storage devices is minimization of mechanical, electrical and other losses. The use of magnetic bearings minimizes mechanical losses by eliminating contact friction. Electromagnetic (e.g., eddy current, ohmic) losses, on the other hand are proportional to the total flux at the bearings [4], [5], [6]. Minimization of the flux is thus essential for designing efficient AMBs for flywheel batteries.

Manuscript received July 22, 2001; revised March 7, 2003. This work was supported in part by AFRL and AFOSR under Award No. F49620-00-1-0374.

P. Tsiotras is with the School of Aerospace Engineering, Georgia Institute of Technology, Atlanta, GA 30332-0150, USA (e-mail: p.tsiotras@ae.gatech.edu).

B.C. Wilson is with the School of Electrical Engineering, Georgia Institute of Technology, Atlanta, GA 30332-0250, USA.

The force generated by an electromechanically activated bearing is a nonlinear function of the flux (or current). As a result, it is customary to linearize the force/flux characteristic by introducing a bias flux (or current). Typical values of the bias current are one-third to one-half of the maximum (saturation) current level for each electromagnet. Since electromagnetic losses at the bearings are proportional to the bias flux, operation with very small or zero bias is imperative for power efficiency. As it will be shown in the sequel, complete elimination of the bias flux results in a linearly uncontrollable system. Zero-bias operation thus calls for nonlinear control techniques. An additional complication arises from the fact that the AMB exhibits a deadzone-like characteristic with reduced force slew-rate capability [7], [8], [9] at zero bias. Standard control designs for a zero-bias AMB result in a singularity manifesting itself as infinite voltage commands when the flux is zero [10], [11].

Several authors have investigated the control problem of an AMB. A comparison between linear and nonlinear operation has been presented by Charara et al [12], [10] and Smith and Weldon [13]. In [10] the authors reported power consumption figures from an experimental apparatus using linear (large bias) and nonlinear (zero bias) controllers. They claim that nonlinear control schemes typically provide dramatic power savings (at the order of 90%) over linear control schemes. Several other nonlinear methods have been investigated for the zero-bias AMB problem. Input-output linearization has been studied in [12], [10], [13], [14], [11]. Sliding mode controllers have been investigated in [10], [15] and [16]. Lévine et al [17] developed an alternative zero-bias control method by studying the differential flatness properties of the system equations. Tsiotras et al [18] have studied stabilization of a zero-bias AMB using control Lyapunov functions. Low-bias techniques for control design have also been studied in [19], [20], [21], [22] and [23]. In [19] the authors applied the integrator-backstepping method to a 2-DOF model and in [20] to a 6-DOF model. In these references a small bias is introduced in order to avoid the singularity when operating at zero bias. An application of the same approach to a large airgap magnetic bearing is given in [21]. Knospe and Yang [23] developed an innovative control scheme for the low-bias control of an AMB. In this approach, the nonlinear equations are quasi-linearized and the system is modelled as a linear parameter-varying (LPV) system. Standard gain-scheduled $\mathcal{H}_\infty$ techniques are then used to stabilize this system. More recently, Knospe [24] has proposed a nonlinear AMB benchmark problem in order to compare different nonlinear control methodologies. Several designs were reported in an invited session during the 2000

American Control Conference [25], [26], [27], [6]. In [25] Lin and Knospe developed an output feedback approach using a high-gain observer. In [26], the authors introduced a passivity-based control approach based on a port-controlled Hamiltonian model. Periodic disturbance rejection has been addressed using a learning control technique in [27]. Variable-bias designs have been investigated in [6] and [28].

In this paper we revisit the zero- and low-bias operations for a 1-DOF AMB. Specifically, we concentrate on alleviating or removing the singularity of zero-bias, voltage-controlled designs when the control flux is zero. This is done by applying a novel integrator-backstepping design for a special class of cascade systems that was originally proposed in [29]. Furthermore, we improve upon current results in the literature by providing a singularity-free design using ideas from passivity theory. We show the improved performance and design flexibility of the proposed designs via numerical simulations. Implementation issues are also discussed at the end of the paper.

The contributions of this work can be summarized as follows: First, a new flux-based model of an AMB is derived using a generalized complementary flux condition. Although this constraint may be a bit more challenging to implement than standard ones, it results in a simple model that is valid both for zero and nonzero bias modes of operation. Second, a new class of zero- and low-bias control laws for AMBs is introduced. The proposed zero-bias control laws are either singularity-free or have a region of singularity that is much smaller than that of standard methods (i.e., using backstepping or feedback linearization).

The notation used in this paper is standard. $\mathbb{R}^n$ denotes the n-dimensional vector space with Euclidean norm $|x| = (\sum^n x_i^2)^{1/2}$. $\mathbb{R}_+$ denotes the non-negative real numbers. $\mathcal{C}^0$ is the space of continuous functions and $\mathcal{C}^1$ is the space of continuously differentiable functions. A symmetric matrix P is positive definite if all its (real) eigenvalues are positive. This fact is denoted by $P > 0$. The directional derivative of the scalar function $V : \mathbb{R}^n \to \mathbb{R}$ in the direction of the vector field $f : \mathbb{R}^n \to \mathbb{R}^n$ at $x \in \mathbb{R}^n$ will be denoted as $L_f V(x) = \frac{\partial V}{\partial x} f(x)$. Given a non-negative integer q, we define $x^{[q]} := \operatorname{sgn}(x) x^q$. Basic properties of the function $x^{[q]}$ are given in the Appendix.

II. The AMB Model

Figure 1 shows a simple schematic of an one-degree-of-freedom AMB. This simplified AMB model consists of two electromagnets used to move a mass m in one dimension. It is assumed that all motion takes place in the x direction and that gravity is not present. To regulate the position x of the mass to zero, the control designer uses the voltage inputs to the electromagnets V_1 and V_2, in order to vary the forces acting on the mass. Since an electromagnet can only produce an attractive force, an electromagnet pair is required to generate forces in the positive and negative x direction. Let Φ_i denote the total flux through the i-th electromagnet. The attractive force generated by each electromagnet is [30]

$$F_i = \frac{\Phi_i^2}{\mu_0 A_g}, \qquad i = 1, 2 \tag{1}$$

where μ_0 is the permeability of free space (= $1.25{\times}10^{-6}\mathrm{H/m}$) and A_g is the area of each electromagnet pole. From Newton's law one obtains

$$m\ddot{x} = \frac{1}{\mu_0 A_g}(\Phi_1^2 - \Phi_2^2) \tag{2}$$

Assume for the moment that the electromagnets are operated with a constant, bias flux $\Phi_0 \geq 0$. The total flux produced by each electromagnet is

$$\Phi_i = \Phi_0 + \phi_i, \qquad i = 1, 2 \tag{3}$$

where ϕ_i is the perturbation (control) flux for the i-th electromagnet. Since the electromagnets produce only an attractive force, there is nothing to be gained by using a "negative flux". Therefore, it will always be assumed that the electromagnets are operated such that $\phi_i \geq 0$ for $i = 1, 2$. Nonetheless, contrary to what is customary done in practice, we do not assume that the bias Φ_0 is large (i.e., $\Phi_0 \ll \phi_i$ is allowed).

From (2) and (3) the equation of motion of the mass is given by

$$\ddot{x} = \frac{1}{\kappa}[\phi_1^2 - \phi_2^2 + 2\Phi_0(\phi_1 - \phi_2)] \tag{4}$$

where $\kappa := m\mu_0 A_g$. The electrical dynamics are given by

$$\dot{\Phi}_i = \dot{\phi}_i = \frac{V_i}{N}, \qquad i = 1, 2 \tag{5}$$

where N is the number of turns of the coil of each electromagnet and V_i is the total voltage applied to each electromagnet[1].

Let us now define the *generalized control flux* $\phi := \phi_1 - \phi_2$ and introduce the following flux-dependent, voltage switching scheme

$$V_1 = \quad v, \quad V_2 = 0 \qquad \text{when} \quad \phi \geq 0 \tag{6a}$$

$$V_2 = -v, \quad V_1 = 0 \qquad \text{when} \quad \phi < 0 \tag{6b}$$

where v is a *generalized control voltage* such that

$$\dot{\phi} = \frac{v}{N} \tag{7}$$

Rewrite now equation (4) as

$$\ddot{x} = \frac{1}{\kappa}(2\Phi_0 + \phi_1 + \phi_2)\phi \tag{8}$$

and assume without loss of generality that $\phi_1(0) \geq \phi_2(0)$. Then $\phi(0) \geq 0$ and by (6) and (5) it follows that for $t \geq 0$

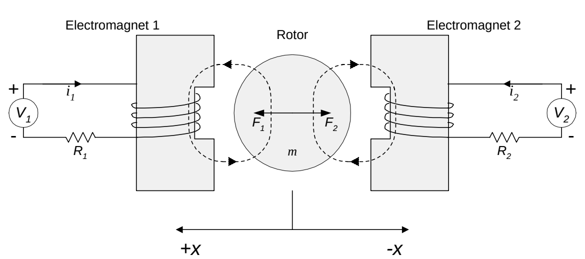

Fig. 1. Schematic of an 1-DOF AMB.

[1] In (5) the coil resistance has been neglected for simplicity. See Section IX-A for the ramifications of this assumption.

we have that $\phi_2 = \phi_2(0)$ and $\phi_1 = \phi + \phi_2(0)$. Subsequently, (8) can be written as

$$\ddot{x} = \frac{1}{\kappa}(2\Phi_0 + 2\phi_2(0) + \phi)\phi, \qquad (\phi \geq 0) \tag{9}$$

If at some point $t_1 > 0$ a switching occurs, then $\phi_1(t_1) = \phi_2(t_1) = \phi_2(0)$. Moreover, from (6) and (5) and for $t \geq t_1$ we have that $\phi_1 = \phi_2(0)$ and $\phi_2 = \phi_2(0) - \phi$. Subsequently, (8) can be written in this case as

$$\ddot{x} = \frac{1}{\kappa}(2\Phi_0 + 2\phi_2(0) - \phi)\phi, \qquad (\phi < 0) \tag{10}$$

The same arguments can be used if another switching occurs and so on.

From the previous simple analysis it follows that the equation of motion (8) under the switching strategy (6) and (5) takes the form

$$\ddot{x} = \frac{1}{\kappa}(2\bar{\Phi}_0\phi + \phi|\phi|) \tag{11}$$

where $\bar{\Phi}_0 := \Phi_0 + \min\{\phi_1(0), \phi_2(0)\}$. As previously mentioned, physical considerations allow us to restrict the set of all realizable trajectories inside the set $\mathcal{S} := \{(x, \dot{x}, \phi_1, \phi_2) \in \mathbb{R}^4 : \phi_i \geq 0,\ i = 1, 2\}$. The following proposition states that the switching scheme (6) is well-defined.

Proposition 1: The set $\mathcal{S}$ is invariant under the switching scheme (6).

Proof: Let $c(t) := \min\{\phi_1(t), \phi_2(t)\}$. Now notice that if $\phi_1 \geq \phi_2$ then $c = \phi_2$ and (6) and (5) imply $\dot{\phi}_2 = \dot{c} = 0$. Similarly, if $\phi_2 \geq \phi_1$ then $c = \phi_1$ and (6) and (5) imply that $\dot{\phi}_1 = \dot{c} = 0$. Therefore $\dot{c} \equiv 0$. It follows that if $c(0) \geq 0$ then $c(t) \geq 0$ for all $t \geq 0$. ■

An immediate consequence of the previous result is that the flux for each electromagnet is never reduced below $\bar{\Phi}_0$ and hence the minimum force generated by each electromagnet is $F_{\min} = \bar{\Phi}_0^2/\mu_0 A_g$.

The introduction of the switching scheme in (6) is motivated from our desire to minimize the control fluxes ϕ_1 and ϕ_2 and hence, eddy and ohmic power losses [24]. When the generalized control flux ϕ is positive, only electromagnet 1 is controlled and when ϕ is negative only electromagnet 2 is controlled. One can think of ϕ as the "excess" flux that needs to be commanded in order to produce the required force. In particular, if at the initial time at least one of the control fluxes is zero, i.e., $\phi_1(0)\phi_2(0) = 0$ (as will be typically the case in practice when operation starts from rest) then at every instant of time at least one of the electromagnets is inactive (its flux is zero). We therefore have the following result as an immediate consequence of Proposition 1.

Proposition 2: The set $\mathcal{S}_0 := \{(x, \dot{x}, \phi_1, \phi_2) \in \mathcal{S} : \phi_1\phi_2 = 0\}$ is invariant under the switching scheme (5)-(6).

Proof: If $(x(0), \dot{x}(0), \phi_1(0), \phi_2(0)) \in \mathcal{S}_0$ then $\min\{\phi_1(0), \phi_2(0)\} = 0$. The claim follows from the fact that $\min\{\phi_1(0), \phi_2(0)\} = \min\{\phi_1(t), \phi_2(t)\}$ for all $t \geq 0$. ■

It is evident from Proposition 2 that for all initial conditions in $\mathcal{S}_0$ the voltage-switching logic (5)-(6) reduces to the following *generalized complementary flux condition* (gcfc) at the flux level

$$\begin{aligned} \phi_1 = \phi, \quad \phi_2 = 0 \quad \text{when} \quad \phi \geq 0 \\ \phi_2 = -\phi, \quad \phi_1 = 0 \quad \text{when} \quad \phi < 0 \end{aligned} \tag{12}$$

This condition implies that the generalized control flux ϕ is generated by only one electromagnet at a time, depending on the direction of the force we need to apply, whereas the control flux in the other electromagnet remains zero.

In this paper we are primarily interested in the stabilization of the AMB mechanical states $(x, \dot{x})$ under low-bias (LB) operation, i.e., when $\bar{\Phi}_0$ is small. As a special case, one obtains a zero-bias (ZB) model by setting $\bar{\Phi}_0 = 0$ in (11). For all subsequent control derivations we will use model (7)-(11) for designing the control law v. Once v is constructed, the voltage is distributed to the actual control inputs V_1 and V_2 activating each electromagnet according to (6). Note that since operation at some non-zero bias is acceptable in this context, we will typically require *asymptotic* stability only with respect to the states x and $\dot{x}$ of the system (4)-(5)[2].

The following result clarifies the relation between equations (7)-(11) and the original AMB model, given by equations (4) and (5).

Theorem 1: Any control law that renders the system (7)-(11) globally asymptotically stable, ensures that:

(i) For all initial conditions in $\mathcal{S}$ the system (4)-(5) is stable.

(ii) For all initial conditions in $\mathcal{S}$, the system (4)-(5) is asymptotically stable with respect to the states $(x, \dot{x})$. Moreover, the fluxes ϕ_1 and ϕ_2 remain bounded and, in addition, $\lim_{t\to\infty} \phi_1(t) = \lim_{t\to\infty} \phi_2(t) = \min\{\phi_1(0), \phi_2(0)\}$.

(iii) For all initial conditions in $\mathcal{S}_0$ the system (4)-(5) is asymptotically stable.

Proof: (i) Let any $\varepsilon > 0$. From the stability of the system (7) and (11) it follows that there exists $\bar{\delta} = \bar{\delta}(\varepsilon) > 0$ such that if $|(x(0), \dot{x}(0))| + |\phi(0)| < \bar{\delta}$ then $|(x(t), \dot{x}(t))| + |\phi(t)| < \varepsilon/2$ for all $t \geq 0$. Consider now all initial conditions in $\mathcal{S}$ such that $|(x(0), \dot{x}(0))| + |\phi(0)| < \bar{\delta}$ and $2\min\{\phi_1(0), \phi_2(0)\} < \varepsilon/2$. Choose $\delta(\varepsilon) := \min\{\bar{\delta}(\varepsilon), \varepsilon/2\}$ and notice that the switching scheme (5)-(6) implies that $\phi_1 = \max\{\phi, 0\} + \bar{c}$ and $\phi_2 = -\min\{\phi, 0\} + \bar{c}$ where $\bar{c} := \min\{\phi_1(0), \phi_2(0)\}$. Hence, for all initial conditions such that $|(x(0), \dot{x}(0))| + |\phi_1(0)| + |\phi_2(0)| = |(x(0), \dot{x}(0))| + |\phi(0)| + 2\min\{\phi_1(0), \phi_2(0)\} < \delta$ we have that $|(x(t), \dot{x}(t))| + |\phi(t)| < \varepsilon/2$ and thus, $|(x(t), \dot{x}(t))| + |\phi_1(t)| + |\phi_2(t)| = |(x(t), \dot{x}(t))| + |\phi(t)| + 2\min\{\phi_1(0), \phi_2(0)\} < \varepsilon/2 + \varepsilon/2 = \varepsilon$ for all $t \geq 0$. Hence (i) follows.

(ii) For all initial conditions in $\mathcal{S}$ asymptotic stability with respect to $(x, \dot{x})$ follows directly from Proposition 1 and the fact that $(x, \dot{x}) \to 0$. Using the fact that $\phi_1 = \max\{\phi, 0\} + \bar{c}$ and $\phi_2 = -\min\{\phi, 0\} + \bar{c}$ and since ϕ is bounded, it follows that both ϕ_1 and ϕ_2 remain bounded. Moreover, since $\phi \to 0$ we have that $\lim_{t\to\infty} \phi_i(t) = \bar{c}$, for $i = 1, 2$.

(iii) First, recall from Proposition 2 that the set $\mathcal{S}_0$ is invariant. Moreover, for all initial conditions in $\mathcal{S}_0$ we have that $\bar{c} = 0$ and the states ϕ_1 and ϕ_2 are related to ϕ via $\phi_1 = \max\{\phi, 0\}$ and $\phi_2 = -\min\{\phi, 0\}$. Since $\phi \to 0$ it follows that $\lim_{t\to\infty} \phi_i(t) = 0$, for $i = 1, 2$. ■

Model (11) is similar to the one used in [33], [23]. It is also somewhat similar to the model of [11], although in [11] the current is used as the electrical state instead of the

[2]This type of stability is also known as partial stability. For the relevant definitions and major results see, for example, [31], [32].

flux. Nonetheless, since the complementarity flux condition is imposed on the generalized control flux (as opposed to the total flux), our approach has the added advantage that it is valid both for zero-bias and low-bias operations.

III. The Role of Bias Flux in AMB Control Design

The main sources of power losses in AMBs are eddy current and ohmic losses. These are directly proportional to the flux through the electromagnets [34], [24]. One can eliminate the bias flux by imposing the following complementary flux condition (cfc) [17], [23], [11]

$$\begin{aligned} \Phi = \ \ \Phi_1, \quad \Phi_2 = 0 \quad \text{when} \quad \Phi \geq 0 \\ \Phi = -\Phi_2, \quad \Phi_1 = 0 \quad \text{when} \quad \Phi < 0 \end{aligned} \tag{13}$$

where only one electromagnet is operated at a time. Here the bias flux Φ_0 is always zero. This is the standard approach for ZB operation in practice. The drawback of ZB operation stems from the fact that since the available force slew rate is controlled by

$$\frac{\mathrm{d}F}{\mathrm{d}t} = \frac{\partial F}{\partial \Phi}\frac{\mathrm{d}\Phi}{\mathrm{d}t} \tag{14}$$

and our ability to change F is controlled by $\frac{\partial F}{\partial \Phi}$[3], the cfc has zero slew rate at the origin.

On the other hand, in order to achieve sufficient force slew rate, a non-zero bias Φ_0 must be used. For a large bias ($\Phi_0 \gg \phi_i$) equation (8) reduces to

$$\ddot{x} \approx \frac{2\Phi_0}{\kappa}\,\phi \tag{15}$$

Thus, the use of a large bias flux leads to an (almost) linear model for the AMB. Consequently, well-established linear control design methodologies can be used. Alternatively, *exact* linearization of (8) is possible by imposing the constraint $\phi_1 = -\phi_2$. This is the *normal* biasing or *constant sum flux* scheme; see [35]. In this case equation (11) reduces to

$$\ddot{x} = \frac{2\Phi_0}{\kappa}\,\phi \tag{16}$$

In the latter case both fluxes are perturbed symmetrically rather than perturbing only a single flux as in the gcfc scheme. However, (16) fails to be controllable at zero bias. Thus, as the bias Φ_0 is reduced, performance of the normal biasing scheme is compromised.

Our approach is somewhat different than the above. First, we do not assume that the bias flux is large compared to the control flux, and hence, the quadratic terms in (8) cannot be ignored. Second, we impose a *generalized* complementarity flux condition (on the generalized control flux) even in the case of a (small) non-zero bias flux. The scheme (6) was motivated by our desire to minimize power losses by operating at low-bias while at the same time being able to recover zero bias as a special case and still remain controllable. Although exact zero-bias operation is rarely desirable in applications due to the limitations already alluded to, we nonetheless insist on a biasing scheme that allows control designs that remain well-behaved as the bias tends to zero. Notice that for ZB operation ($\bar{\Phi}_0 = 0$), our AMB model reduces to the standard AMB model subject to the cfc constraint (13) and remains (nonlinearly) controllable. Moreover, the gcfc force F given by equation (11) has a slew rate $\frac{\partial F}{\partial \phi}$ that is proportional to the bias level.

[3]It is assumed that our ability to change Φ is independent of the particular biasing scheme. This is a realistic assumption if the same amplifiers are used to drive the coils of the AMB in each case.

IV. Problem Statement

In order to work with a system having the minimum number of parameters, we find it convenient to introduce the following non-dimensionalized state and control variables along with a non-dimensionalized time

$$\begin{gathered} x_1 := \frac{x}{g_0}, \quad x_2 := \frac{\dot{x}}{\Phi_{\rm sat}\sqrt{g_0/\kappa}}, \quad x_3 := \frac{\phi}{\Phi_{\rm sat}}, \\ u := \frac{v\sqrt{g_0\kappa}}{N\Phi_{\rm sat}^2}, \quad \tau := t\frac{\Phi_{\rm sat}}{\sqrt{g_0\kappa}} \end{gathered} \tag{17}$$

where g_0 is the nominal air-gap and $\Phi_{\rm sat}$ is the value of the saturation (maximum) flux. Notice that since (Flux) = (Flux density) $\times$ (Cross-sectional Area of Core), $\Phi_{\rm sat}$ can be readily calculated by the maximum flux density of the electromagnetic core (typically 1.2–2 Tesla).

In terms of these non-dimensionalized variables, the system (11)-(7) can be written in state-space form as follows

$$x_1' = x_2 \tag{18a}$$
$$x_2' = \epsilon x_3 + x_3|x_3| := f_2(x_3) \tag{18b}$$
$$x_3' = u \tag{18c}$$

where $\epsilon := 2\bar{\Phi}_0/\Phi_{\rm sat}$ and where prime denotes differentiation with respect to τ. Notice that $\epsilon \geq 0$ for all initial conditions in $\mathcal{S}$. Low-bias operation in this context therefore implies that $\epsilon \ll 1$, while zero bias implies that $\epsilon = 0$.

With a slight abuse of notation, we revert to the use of dot in (18) to denote differentiation with respect to the non-dimensionalized time and re-write equations (18) in the following control-affine form

$$\dot{x} = f(x) + g(x)u \tag{19}$$

with vector fields $f : \mathbb{R}^3 \to \mathbb{R}^3$ and $g : \mathbb{R}^3 \to \mathbb{R}^3$ given by

$$f(x) := \begin{bmatrix} x_2 \\ \epsilon x_3 + x_3^{[2]} \\ 0 \end{bmatrix}, \qquad g(x) := \begin{bmatrix} 0 \\ 0 \\ 1 \end{bmatrix} \tag{20}$$

and where the notation $x_3^{[2]} := \mathrm{sgn}(x_3)x_3^2 = x_3|x_3|$ has been adopted.

Our goal is to find a control law $u : \mathcal{D} \to \mathbb{R}$ such that

(i) the closed-loop system $\dot{x} = \tilde{f}(x) := f(x) + g(x)u(x)$ has an isolated equilibrium at the origin
(ii) the origin is asymptotically stable for all $x(0) \in \mathcal{D}$
(iii) The domain of definition $\mathcal{D} \subseteq \mathbb{R}^3$ of the control law $u(x)$ is as large as possible

According to the discussion in the previous section, in order to reduce the power losses one would like–ideally–to set $\epsilon = 0$. However, this approach introduces several difficulties. First, from (20) it is seen that for $\epsilon = 0$ the system is linearly uncontrollable. Second, for zero-bias, the AMB has no force-slew rate capability when the flux is zero [7], [9], [8]. The force vs. flux curve has a zero slope at $\phi = 0$ and the AMB cannot respond fast enough to force commands. As a result, most control design techniques for zero-bias AMBs will command a very high (even infinite) voltage when the flux is zero. The ZB control design for a voltage-controlled AMB is thus far from trivial. It is the purpose of this paper to revisit the ZB control design for an AMB and propose a new class of control laws which are valid both for LB and ZB operation.

V. Control Design via Standard Backstepping

In the next section we propose a new class of control laws for LB/ZB operation of an AMB. From (20) it is evident that the linearization is not controllable for $\epsilon = 0$. Purely nonlinear control techniques (i.e., techniques that do not depend on the linearization of (20)) must therefore be used instead. To better appreciate the contributions of the present work, we next briefly demonstrate the difficulties encountered when one applies a standard backstepping methodology to design a controller for a bearing without bias flux.

To this end, notice that the system of equations (19)-(20) have a simple cascaded structure as follows

$$\dot{z} = f_0(z, y) \tag{21a}$$
$$\dot{y} = u \tag{21b}$$

where we partition the state variables x_1, x_2, and x_3 into the mechanical subsystem variables $z = [z_1, z_2]^T := [x_1, x_2]^T$ and the electrical subsystem variables $y = x_3$. With these definitions, $f_0(z, y) := [z_2,\ f_2(y)]^T$ and $f_2(y) = \epsilon y + y^{[2]}$. A common technique for the stabilization of cascaded systems is backstepping. In this approach, one views the state-variable y as the control input to the $f_0(z, y)$ subsystem and then one assigns the dynamics for y via the integrator (21b). To this end, first note that if one chooses y such that

$$f_2(y) = \sigma(z) := -k_1 z_1 - k_2 z_2 \tag{22}$$

the z-subsystem is feedback linearized. In this case, the z-subsystem is given by $\dot{z} = Az$ where

$$A := \begin{bmatrix} 0 & 1 \\ -k_1 & -k_2 \end{bmatrix} \tag{23}$$

For $k_1 > 0$ and $k_2 > 0$ the matrix A is Hurwitz. Let us now introduce the function $u_0 : \mathbb{R}^2 \to \mathbb{R}$ such that $f_2(u_0(z)) = \sigma(z)$ for all $z \in \mathbb{R}^2$. It can be easily verified that

$$u_0(z) := -\tfrac{1}{2}\mathrm{sgn}(\sigma(z))(\epsilon - \sqrt{\epsilon^2 + 4|\sigma(z)|}) \tag{24}$$

For $\epsilon = 0$ this function reduces to

$$u_0(z) = \mathrm{sgn}(\sigma)|\sigma|^{\frac{1}{2}} \tag{25}$$

If one now tries to implement the *virtual control law* $u_0(z)$ via (21b) one immediately faces the problem of the non-Lipschitz continuity of the inverse of the function $f_2(y)$ at the origin when $\epsilon = 0$. If, for instance, as usual one defines the error variable $\eta = f_2(y) - \sigma(z)$ one ends up with the backstepping control law

$$u(z, y) = \left(\frac{\partial f_2}{\partial y}\right)^{-1} \left[\frac{\partial \sigma}{\partial z}(Az + b\eta) - 2b^T P z - \gamma\eta\right], \quad \gamma > 0 \tag{26}$$

where $P > 0$ satisfies the matrix inequality (such a P always exists since A is Hurwitz)

$$A^T P + PA < 0 \tag{27}$$

Using the Lyapunov function

$$V(z, y) = z^T P z + \tfrac{1}{2}\eta^2 \tag{28}$$

it can be easily shown that this control law globally asymptotically stabilizes the complete system. However, the control law (26) is singular at $y = 0$ for $\epsilon = 0$. Indeed, since

$$\left(\frac{\partial f_2}{\partial y}\right)^{-1} = \frac{1}{2|y| + \epsilon} \tag{29}$$

the control law (26) is not defined at $x_3 = y = 0$ for the case of zero-bias flux.

The issue of singularity with this standard backstepping control design approach is well-known in the literature. Several ad hoc methods to remedy this situation have been proposed. In [10] and [11][4], for instance, for the ZB case the authors replace $1/2|y|$ with $1/(2|y| + \delta)$ where $\delta > 0$ is a very small number in the calculation of $(\partial f_2/\partial y)^{-1}$. A similar small bias term has been added in the backstepping designs of [19] and [20] to avoid this singularity.

It should come as no surprise that the singularity is still present even if one introduces an alternative definition for the error. If, for example, we let $\eta = y - u_0(z)$ the z-subsystem can be written as

$$\dot{z} = Az + b(z, y)\eta \tag{30}$$

where $b(z, y) = [0,\ \pi(z, y)]^T$, and where $\pi(z, y) \in \mathcal{C}^0$ satisfies $f_2(y) = f_2(u_0(z)) + \pi(z, y)\eta$. For example, one may choose[5]

$$\pi(z, y) := \frac{f_2(y) - f_2(u_0(z))}{y - u_0(z)} \tag{31}$$

Using the same Lyapunov function candidate as in (28) it can be shown that the choice of the control law

$$u(z, y) = \frac{1}{\sqrt{\epsilon^2 + 4|\sigma(z)|}} \left(\frac{\partial \sigma}{\partial z}\right) \Big(Az + b(z, y)\eta\Big) - 2b^T(z, y)Pz - \gamma\eta, \qquad \gamma > 0 \tag{32}$$

results in a globally asymptotically closed-loop system for all $\epsilon \geq 0$. The control law (32) is bounded for all $\epsilon > 0$. For $\epsilon = 0$ this control law exhibits a singularity when $\sigma(z) = 0$.

[4]In these references the current is used instead of the flux as a state variable. However, the approach is essentially the same.

[5]Notice that $\pi(z, y) \in \mathcal{C}^0$ for all $\epsilon \geq 0$ since $f_2 \in \mathcal{C}^1$.

VI. Low- and Zero-Bias Control Design

In the sequel we use ideas from the theory of control Lyapunov functions (clf's) and the extended integrator backstepping techniques of [29] to design a stabilizing control law for (18).

Definition 1: A function $V : \mathbb{R}^n \to \mathbb{R}_+$ is a *control Lyapunov function* (clf) for the system $\dot{x} = f(x) + g(x)u$ if it satisfies the following properties:

(i) V is positive definite
(ii) $V \in \mathcal{C}^1$
(iii) V is radially unbounded, and
(iv) $L_f V(x) < 0$ for all $x \neq 0$ such that $L_g V(x) = 0$

Control Lyapunov functions have been instrumental for global stabilization of nonlinear systems (see, for instance, [36] and [37]). Generally speaking, if a system has a clf, then there exists a control law (with certain smoothness properties) that renders the system asymptotically stable. Sontag [38] has proposed an explicit expression for such a control law that stabilizes a system using its clf. Sontag's formula is

$$u = \begin{cases} 0, & L_g V(x) = 0 \\ -\dfrac{L_f V + \sqrt{L_f V^2 + L_g V^4}}{L_g V}, & \text{otherwise} \end{cases} \tag{33}$$

This control law is smooth in $\mathbb{R}^n \backslash \{0\}$ and it is continuous at the origin if and only if the clf satisfies the *small control property* [36].

A. Clf's for Cascaded Systems

The main drawback of the clf approach is that, generally, it is difficult to determine if a system possesses a clf. However, for systems that have a cascaded structure, there exist constructive algorithms to find clf's. To this end, consider a cascade system of the form as in (21) with $z \in \mathbb{R}^{n-1}$ and $y \in \mathbb{R}$. Assume that there exists a control law $u_0(z)$ with corresponding Lyapunov function $V_0(z)$, so that $z = 0$ is a globally asymptotically stable (GAS) equilibrium of the closed-loop system $\dot{z} = f_0(z, u_0(z))$. Under some mild hypotheses, the function

$$V(z, y) = \tfrac{1}{2}(y - u_0(z))^2 + V_0(z) \tag{34}$$

is then a clf for the cascade system [36]. This construction may not work if the stabilizing control law $u_0(z)$ for the z-dynamics is not smooth enough, since in this case the function V may not be $\mathcal{C}^1$; see property (ii) of Definition 1. Notice that this is precisely the situation with the control $u_0(z)$ in (25) for the case of an AMB in ZB operation.

To remedy this difficulty, we use the results of extended backstepping design of Praly et al [29]. According to [29], one introduces a "desingularizing" function $\psi(z, y) \in \mathcal{C}^0$ so that V has the required smoothness properties. The function $\psi(z, y)$ is chosen such that $\psi(z, y) = 0$ implies $y = u_0(z)$. Related to the function $\psi(z, y)$ is the function $\Psi \in \mathcal{C}^1$ defined by

$$\Psi(z, y) := \int_0^y \psi(z, q) \mathrm{d}q \tag{35}$$

where, for all $z \in \mathbb{R}^{n-1}$, $\Psi(z, y) \to \infty$ as $|y| \to \infty$. The form of the clf is then given by

$$V(z, y) = \Psi(z, y) - \Psi(z, u_0(z)) + \beta V_0(z)^\alpha, \quad \beta > 0 \tag{36}$$

where α is such that $V_0(z)^\alpha \in \mathcal{C}^1$.

Assuming a Lyapunov function $V_0(z)$ for the z-subsystem in (21a) is known, the problem of finding a clf for (21) is reduced to one of finding a desingularizing function ψ. Once the clf is known, one may use Sontag's formula (33) to construct a controller. Alternatively, one may use the control law in the following lemma.

Lemma 1 ([29]): Given a system as in (21), assume that $u_0(z)$ is a control law that asymptotically stabilizes (21a) and $V_0(z)$ is the corresponding Lyapunov function. Consider the positive definite function $V(z, y)$ given in (36). This function is a proper clf for (21) and the following choice of the control law will globally asymptotically stabilize (21)

$$\begin{aligned} u(z, y) = \left(\frac{\partial \Psi}{\partial y}(z, y)\right)^{-1} \Big\{ &\left(\frac{\partial \Psi}{\partial z}(z, u_o(z)) - \frac{\partial \Psi}{\partial z}(z, y)\right) f_0(z, y) \\ &+ \alpha\beta V_0(z)^{\alpha-1}\Big(L_{f_0(z,u_0(z))} V_0(z) - L_{f_0(z,y)} V_0(z)\Big)\Big\} \\ &- \Theta(z, y) \end{aligned} \tag{37}$$

where $\Theta(z, y) \in \mathcal{C}^0$ and has the same sign as $\psi(z, y)$.

B. Low- and Zero-Bias Control of an AMB

Next, we apply the result of Lemma 1 in order to find a stabilizing control law for (18). The first step is to find a stabilizing controller u_0 and a Lyapunov function V_0 for the z-dynamics. Let us choose u_0 as in (24) and $V_0 = z^T P z$ where P as in (27). With $u_0(z)$ and $V_0(z)$ in hand, one needs to determine the desingularizing function. Since $u_0(z)^{[2p]} \in \mathcal{C}^1$ for $p \geq 1$ and for all $\epsilon \geq 0$, the following desingularizing function is proposed

$$\psi(z, y) = \epsilon\,(y - u_0(z)) + y^{[2p]} - u_0(z)^{[2p]}, \qquad p \geq 1 \tag{38}$$

It can be shown that ψ is continuous and that $\psi(z, y) = 0$ implies that $y = u_0(z)$. The function $\psi(z, y)$ is integrated with respect to y to obtain $\Psi(z, y)$ and $\Psi(z, u_0(z))$. A simple calculation shows that

$$\Psi(z, y) = \int_0^y \psi(z, q)\, \mathrm{d}q = \frac{\epsilon}{2} y^2 - \epsilon y u_0(z) + \frac{y^{[2p+1]}}{2p+1} - y u_0(z)^{[2p]} \tag{39}$$

and

$$\Psi(z, u_0(z)) = -\frac{\epsilon}{2} u_0(z)^2 - \frac{2p}{2p+1} u_0(z)^{[2p+1]} \tag{40}$$

Inserting equations (39) and (40) into (36), one obtains

$$\begin{aligned} V(z, y) = &\frac{\epsilon}{2}\,(y - u_0(z))^2 + \frac{y^{[2p+1]}}{2p+1} - y u_0(z)^{[2p]} \\ &+ \frac{2p}{2p+1} u_0(z)^{[2p+1]} + \beta V_0(z)^\alpha \end{aligned} \tag{41}$$

with $p \geq 1$, $\beta > 0$, and $\alpha > \frac{1}{2}$, is an appropriate clf for the system (18). The value of $\alpha > \frac{1}{2}$ ensures that $V_0(z)^\alpha \in \mathcal{C}^1$. Given the clf in (41), one applies Lemma 1 to obtain the following control law for (18).

Proposition 3: Let $k_1 > 0$ and $k_2 > 0$ and let P be a positive definite matrix such that $A^T P + PA < 0$. Let $V_0 = z^T P z$ and consider the control law

$$u = \Big(\epsilon x_3 + x_3^{[2p]} - \epsilon u_0 - u_0^{[2p]}\Big)^{-1} \times \Big\{ \frac{p\,(\epsilon - \sqrt{\epsilon^2 + 4|\sigma|})^{2p-1} - 2^{2p-2}\epsilon}{2^{2p-2}\sqrt{\epsilon^2+4|\sigma|}} \times (x_3 - u_0)\Big(k_1 x_2 + k_2 f_2(x_3)\Big) + \alpha\beta V_0^{\alpha-1}\frac{\partial V_0}{\partial x_2}\Big(f_2(u_0(z)) - f_2(x_3)\Big)\Big\} - \Theta(x) \quad (42)$$

where $p \geq 1$, $\beta > 0$, $\alpha > \frac{1}{2}$, and where $\Theta(x)$ has the same sign as $\epsilon(x_3 - u_0) + x_3^{[2p]} - u_0^{[2p]}$ with $u_0(\sigma(z))$ and $\sigma(z)$ defined in (24) and (22), respectively. This control law globally asymptotically stabilizes system (18).

Proof: The proposition follows from Lemma 1 by noticing that

$$\frac{\partial \Psi(z,y)}{\partial z} = -y\frac{\partial u_0(z)^{[2p]}}{\partial z} - \epsilon y \frac{\partial u_0(z)}{\partial z}$$
$$\frac{\partial \Psi(z,u_0(z))}{\partial z} = -\frac{2p}{2p+1}\frac{\partial u_0(z)^{[2p+1]}}{\partial z} - \epsilon u_0 \frac{\partial u_0(z)}{\partial z}$$

A straightforward calculation shows that

$$\frac{\partial u_0}{\partial z} = \frac{1}{\sqrt{\epsilon^2+4|\sigma|}}\frac{\partial \sigma}{\partial z}$$

Moreover, since

$$\frac{\partial}{\partial z}u_0^{[2p]} = -p\,\frac{(\epsilon - \sqrt{\epsilon^2+4|\sigma|})^{2p-1}}{2^{2p-2}\sqrt{\epsilon^2+4|\sigma|}}\frac{\partial\sigma}{\partial z}$$
$$\frac{\partial}{\partial z}u_0^{[2p+1]} = \frac{2p+1}{2}\mathrm{sgn}(\sigma)\frac{(\epsilon - \sqrt{\epsilon^2+4|\sigma|})^{2p}}{2^{2p-1}\sqrt{\epsilon^2+4|\sigma|}}\frac{\partial\sigma}{\partial z}$$

one obtains,

$$\frac{\partial \Psi(z,u_0(z))}{\partial z} - \frac{\partial \Psi(z,y)}{\partial z} = \left(-\frac{p\,(\epsilon - \sqrt{\epsilon^2+4|\sigma|})^{2p-1}}{2^{2p-2}\sqrt{\epsilon^2+4|\sigma|}} + \frac{\epsilon}{\sqrt{\epsilon^2+4|\sigma|}}\right)(y - u_0)\frac{\partial\sigma}{\partial z}$$

Furthermore, the difference between the Lie derivative terms in (37) can be written as

$$L_{f_0(z,u_0(z))}V_0(z) - L_{f_0(z,y)}V_0(z) = \frac{\partial V_0(z)}{\partial z_2}(f_2(u_0(\sigma)) - f_2(y))$$

Inserting the last two equations into (37) one obtains (42). ■

Since the function $x^{[2p]}$ is odd and one-to-one, a simple choice for Θ that satisfies the requirements of the previous proposition is

$$\Theta(x) = \gamma(x_3 - u_0(z)), \qquad \gamma > 0 \quad (43)$$

The control law in (42) simplifies to the one reported in [18] for zero-bias mode. Setting $\epsilon = 0$ in (42) one obtains

$$u = -(u_0^{[2p]} - x_3^{[2p]})^{-1}\Big\{p\,u_0^{2p-2}(u_0 - x_3)(k_1 x_2 + k_2 x_3^{[2]}) + \alpha\beta V_0^{\alpha-1}\frac{\partial V_0}{\partial x_2}(u_0^{[2]} - x_3^{[2]})\Big\} - \Theta(x) \quad (44)$$

where u_0 as in (25). We remind the reader that once the clf (41) is known, one can also use (33) to construct a stabilizing control law. The added benefit of using (44) instead, is that one can ensure that the closed-loop system is homogeneous of degree zero with respect to the dilation[6] $\Delta_\lambda(x) = (\lambda^2 x_1, \lambda^2 x_2, \lambda x_3)$ when $\alpha = (2p+1)/4$ and for all $p \geq 1$. Moreover, the larger the p, the smoother the control law on $\mathbb{R}^n \backslash \{0\}$. Thus, p can be used as a "tuning" parameter to smooth the control law away from the origin.

Remark 1: The control law in (44) is not defined on the set $\mathcal{D}_1 := \{x \in \mathbb{R}^3 |\ x_3 = u_0(z) = 0\}$. By comparison, the standard backstepping controllers (26) and (32) are singular on the sets $\mathcal{D}_2 := \{x \in \mathbb{R}^3 |\ x_3 = 0\}$ and $\mathcal{D}_3 := \{x \in \mathbb{R}^3 |\ u_0(z) = 0\}$, respectively. Thus, the domain of definition of the proposed control (44) is much larger than that of a typical backstepping design. In fact, the singularity sets $\mathcal{D}_2$ and $\mathcal{D}_3$ are planes in $\mathbb{R}^3$ while $\mathcal{D}_1 = \mathcal{D}_2 \cap \mathcal{D}_3$ is a line in $\mathbb{R}^3$. Note, however, that in low bias mode the control law in (42) is always well-defined and $\mathcal{D} = \mathbb{R}^3$.
The next section shows that one may use passivity arguments to design ZB control laws that are nonsingular everywhere.

VII. Passivity-Based Control Design

In this section we show that the simple control law

$$u_0(z) = -k_1 z_1 - k_2 z_2 \quad (45)$$

where $k_1 > 0$, $k_2 > 0$, globally asymptotically stabilizes (21a) via the virtual input y. Since the control law in (45) is linear, it can be implemented directly via (21b) using standard backstepping. In order to show that (45) is a stabilizing control law for (21b) we use ideas from the theory of dissipative/passive systems [37], [41], [42].

A. Stabilization of the Mechanical Subsystem

We first focus on the stabilization of the mechanical subsystem dynamics of the AMB which is described by the equations

$$\dot{z}_1 = z_2 \quad (46a)$$
$$\dot{z}_2 = f_2(y) = \epsilon y + y^{[2]} \quad (46b)$$

Lemma 2: Consider the z_2-equation of the mechanical subsystem dynamics (46b) with

$$y = -k_2 z_2 + r_1, \qquad k_2 > 0 \quad (47)$$

This system is dissipative with input r_1 and output z_2 with respect to the supply rate $w_1(r_1, z_2) = z_2 f_2(r_1)$. Equivalently, it is passive from input $f_2(r_1)$ to output z_2.

Proof: Consider the storage function $S_1(z_2) = \frac{1}{2}z_2^2$. Calculating its time derivative one obtains $\dot{S}_1 = z_2\dot{z}_2 = z_2 f_2(r_1 - k_2 z_2)$. If $z_2 = 0$ then $\dot{S}_1 = 0$ and the system is trivially dissipative. If $z_2 \neq 0$ (assume without loss of generality that $z_2 < 0$), by the Mean Value Theorem [43] there exists $\xi \in (r_1, r_1 - k_2 z_2)$ such that $f_2(r_1 - k_2 z_2) = f_2(r_1) - k_2 f_2'(\xi) z_2$. Let $\delta(\xi) ;= f_2'(\xi) = \epsilon + 2|\xi|$. If $\epsilon > 0$ then $\delta(\xi) \geq \epsilon > 0$ for all $\xi \in \mathbb{R}$. For the zero-bias case, $\epsilon = 0$

[6] For the relevant definitions on homogeneous vector fields and dilation operators, as well as their properties, see for example [39] and [40]

and $\delta(\xi) = 2|\xi| \geq 0$. Moreover, if $z_2 \neq 0$ then necessarily $\xi \neq 0$ and hence $\delta(\xi) > 0$. To see this, assume instead that $\xi = 0$. Then $f_2(r_1 - k_2 z_2) = f_2(r_1)$ and since the function f_2 is one-to-one, this implies that $r_1 - k_2 z_2 = r_1$ or that $z_2 = 0$, a contradiction.

Hence we have shown that

$$\begin{aligned}\dot{S}_1 &= z_2(f_2(r_1) - k_2\delta(\xi)z_2) \\ &= z_2 f_2(r_1) - k_2\delta(\xi)z_2^2 \leq z_2 f_2(r_1)\end{aligned}$$

for all r_1 and z_2. Therefore the system (46b)-(47) is passive from input $f_2(r_1)$ to output z_2. ■

The integrator (46a) is clearly dissipative (in fact, lossless) from z_2 to z_1 with respect to the supply rate $w(z_1, z_2) = z_1 z_2$. Next, we show that dissipativity still holds if one chooses a slightly different supply rate.

Lemma 3: The system (46a) from input z_2 to output z_1 is dissipative (lossless) with respect to the supply rate $w(z_1, z_2) = f_2(k_1 z_1) z_2$. Equivalently, it is passive from input z_2 to output $f_2(k_1 z_1)$.

Proof: Let the storage function

$$S_2(z_1) = \frac{1}{k_1}\int_0^{k_1 z_1} f_2(\tau)\,\mathrm{d}\tau$$

This is positive definite since f_2 is an odd function. Calculating its derivative yields

$$\dot{S}_2 = f_2(k_1 z_1)\dot{z}_1 = f_2(k_1 z_1) z_2$$

which gives the desired result. ■

Lemmas 2 and 3 motivate one to choose the following expression for the input r_1 in (47)

$$r_1 = -k_1 z_1, \qquad k_1 > 0 \tag{48}$$

The previous choice for r_1 results in a negative feedback

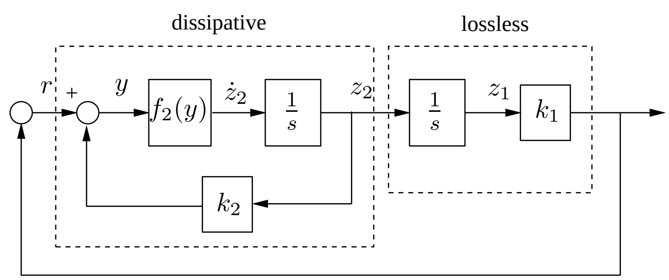

Fig. 2. Overall feedback interconnection.

interconnection of a dissipative with a lossless system. The overall feedback interconnection is shown in Fig. 2. Under some mild assumptions, it is expected that this interconnection will be GAS. This is indeed true as shown in the next proposition.

Proposition 4: The system (46) with the control law

$$y = u_0(z) = -k_1 z_1 - k_2 z_2 \tag{49}$$

where $k_1 > 0$ and $k_2 > 0$ is globally asymptotically stable.

Proof: Consider the Lyapunov function candidate

$$V_1 = S_1(z_2) + S_1(z_1) = \frac{1}{2}z_2^2 + \frac{1}{k_1}\int_0^{k_1 z_1} f_2(\tau)\,\mathrm{d}\tau \tag{50}$$

Clearly, this is a positive definite function. Calculating the time derivative of V_1 along the trajectories of (46) one obtains, following similar arguments as in the proof of Lemma 2

$$\begin{aligned}\dot{V}_1 &= -z_2 f_2(k_1 z_1 + k_2 z_2) + \frac{1}{k_1} f_2(k_1 z_1) k_1 z_2 \\ &= -z_2 f_2(k_1 z_1) - \delta(\xi) k_2 z_2^2 + z_2 f_2(k_1 z_1) \\ &= -\delta(\xi) k_2 z_2^2 \leq 0\end{aligned}$$

Recall that $\delta(\xi) \geq 0$ and $\delta(\xi) = 0$ if and only if $\epsilon = 0$ and $z_2 = 0$. If $z_2 = 0$ identically then $\dot{z}_2 = 0$. It follows that $f_2(k_1 z_1) = 0$ and hence $z_1 = 0$. Thus, the only invariant set of the system (46)-(49) is $z_1 = z_2 = 0$. Since V_1 is radially unbounded and $\dot{V}_1 \leq 0$, all system trajectories are bounded. Using LaSalle's Theorem [44], it follows that the system is GAS. ■

Energy considerations lead to the following alternative proof of stability of the system (46b) with control law (49). Consider the following positive-definite, radially unbounded Lyapunov function candidate[7]

$$V_2 = \frac{k_1}{2} z_2^2 + \int_0^{u_0(z)} f_2(\tau)\,\mathrm{d}\tau \tag{51}$$

where $u_0(z)$ as in (49). Calculating the time derivative of V_2 along the trajectories of (46) one obtains,

$$\begin{aligned}\dot{V}_2 &= k_1 z_2 f_2(u_0(z)) + f_2(u_0(z))(-k_1 z_2 - k_2 f_2(u_0(z))) \\ &= -k_2 f_2^2(u_0(z)) \leq 0\end{aligned}$$

Since V_2 is radially unbounded all solutions are bounded. If $u_0(z) = 0$ identically, then $\dot{u}_0(z) = 0$. The last condition implies that $\dot{u}_0(z) = -k_1\dot{z}_1 - k_2\dot{z}_2 = -k_1 z_2 - k_2 f_2(u_0(z)) = 0$ which together with $u_0(z) = 0$ implies that $z_2 = 0$. Hence also $z_1 = 0$ and the origin is the only invariant subset inside the set $\{z \in \mathbb{R}^2 : \dot{V}_2 = 0\}$. Global asymptotic stability follows immediately from LaSalle's Theorem.

B. Stabilization of the Cascade

To complete the stabilization of the overall system it suffices to implement the flux command (49) via the integrator (21b). To this end, let the new state variable $\eta = y - u_0(z)$ and rewrite the system dynamics as follows

$$\begin{aligned}\dot{z}_1 &= z_2 && \text{(52a)} \\ \dot{z}_2 &= f_2(\eta + u_0(z)) && \text{(52b)} \\ \dot{\eta} &= u + k_1 z_2 + k_2 f_2(y) && \text{(52c)}\end{aligned}$$

Proposition 5: Consider the system (52) and let the control law

$$u = -k_1 z_2 - k_2 f_2(y) - \gamma\eta \tag{53}$$

where k_1, k_2 and γ are some positive constants. Then the closed-loop system is locally asymptotically stable.

Proof: Using (53) the closed-loop system takes the form

$$\begin{aligned}\dot{z}_1 &= z_2 && \text{(54a)} \\ \dot{z}_2 &= f_2(u_0(z)) + \tilde{\pi}(z,\eta)\eta && \text{(54b)} \\ \dot{\eta} &= -\gamma\,\eta && \text{(54c)}\end{aligned}$$

[7]This Lyapunov function was suggested by A. Teel and M. Arcak [45].

where $\tilde{\pi}(z,\eta) = \pi(z,\eta+u_0(z))$ and $\pi(z,y)$ as in (31). The result follows by linearizing the closed-loop system (52)-(53) and showing that the linearized system matrix is Hurwitz. ■

Global asymptotic stability cannot be ensured with the control law (53) without extra conditions. For example, if one could show that the system (54a)-(54b) is Input-to-State Stable (ISS) from input η to the state z then global asymptotic stability would follow as a result of a cascade interconnection of the globally exponentially stable system $\dot{\eta} = -\gamma\,\eta$ with an ISS system [37].

Global asymptotic stability can still be ensured if one chooses a slightly different control law.

Proposition 6: The system (52) with the control law

$$u = -k_1 z_2 - k_2 f_2(y) - z_2\pi(z,y) - \gamma\eta \tag{55}$$

where k_1, k_2, γ are positive constants, is GAS.

Proof: Consider the Lyapunov function $V = V_1 + \frac{1}{2}\eta^2$ where V_1 as in equation (50). The derivative of V is

$$\begin{aligned}\dot{V} &= z_2 f_2(y) + f_2(k_1 z_1) z_2 + \eta\dot{\eta}\\ &= z_2 f_2(u_0(z)) + z_2\pi(z,y)\eta + f_2(k_1 z_1) z_2\\ &\quad +\eta(u + k_1 z_2 + k_2 f_2(y))\\ &= -\delta(\xi) k_2 z_2^2 + \eta(u + k_1 z_2 + k_2 f_2(y) + z_2\pi(z,y))\end{aligned}$$

where $\xi \in (-k_1 z_1, -k_1 z_1 - k_2 z_2)$. Using the control law (55) the last inequality yields,

$$\dot{V} = -\delta(\xi) k_2 z_2^2 - \gamma\eta^2 \tag{56}$$

Recall that $\delta(\xi) = f_2'(\xi) \geq 0$ and that $\delta(\xi) > 0$ for all $\xi \in \mathbb{R}$ if $\epsilon > 0$. In case $\epsilon = 0$ then $\delta(\xi) = 0$ if and only if $z_2 = 0$. In either case, (56) implies that the origin is a stable equilibrium point and that all trajectories are bounded. To show asymptotic stability, assume that $\eta = 0$ and that $z_2 = 0$ over a non-trivial interval of time. Then $\dot{z}_2 = 0$ as well, and from (52b) it follows that $u_0(z) = 0$. This, along with $z_2 = 0$ implies that $z_1 = 0$. Therefore, the only invariant subset inside the set $\{(z_1, z_2, \eta) \in \mathbb{R}^3 : \dot{V} = 0\}$ is the origin. From LaSalle, it follows that the origin is asymptotically stable. GAS follows from the radial unboundedness of V. ■

Alternatively, we have the following result using the Lyapunov function in (51).

Proposition 7: The system (52) with the control law

$$u = -k_1 z_2 - k_2 f_2(y) - \pi(z,y)(k_1 z_2 - k_2 f_2(u_0(z))) - \gamma\eta \tag{57}$$

where k_1, k_2, γ are positive constants, is GAS.

Proof: Let $V = V_2 + \frac{1}{2}\eta^2$ where V_2 as in (51). Calculating the derivative of V, yields

$$\begin{aligned}\dot{V} &= k_1 z_2 f_2(y) - f_2(u_0(z))(k_1 z_2 + k_2 f_2(y)) + \eta\dot{\eta}\\ &= k_1 z_2 (f_2(u_0(z)) + \eta\pi(z,y)) - k_1 z_2 f_2(u_0(z))\\ &\quad -k_2 f_2(u_0(z))(f_2(u_0(z)) + \eta\pi(z,y)) + \eta\dot{\eta}\\ &= -k_2 f_2^2(u_0(z)) + \eta\Big(u + k_1 z_2 + k_2 f_2(y)\\ &\quad +\pi(z,y)(k_1 z_2 - k_2 f_2(u_0(z)))\Big)\end{aligned}$$

Letting u as in (57) yields $\dot{V} = -k_2 f_2^2(u_0(z)) - \gamma\eta^2 \leq 0$. It follows that the origin is stable in the sense of Lyapunov and that all trajectories are bounded. Global asymptotic stability follows using a standard LaSalle argument. ■

VIII. Numerical Examples

This section illustrates the performance of the above control laws when applied to a specific AMB modelled as in (18). The specifications for this AMB are shown in Table I. The constant g_0 is the distance from each electromagnet to the rotor when the rotor is centered at $x = 0$; see Fig. 1. These specifications were taken from [4].

TABLE I
AMB specifications

Symbols	Meaning
$N = 321$	♯ of turns in coil
$m = 4.5$ kg	effective mass of rotor
$\Phi_{\rm sat} = 200\ \mu$Wb	saturation flux
$A_g = 137$ mm^2	electromagnet pole area
$g_0 = 0.33$ mm (13 mils)	nominal width of airgap (when $x = 0$)
$x_{\max} = 0.254$ mm (10 mils)	maximum displacement

Numerical simulations were conducted for various combinations of the control parameters. The initial conditions for all the simulations are $(x(0), \dot{x}(0), \phi(0)) = (x_{\max}, 0, 0)$. In all simulations it was assumed that both electromagnets start from rest and thus $\phi_1(0) = \phi_2(0) = 0$. This allows us to test the performance of the control laws in zero bias by setting $\bar{\Phi}_0 = \Phi_0 = 0$.

Figure 3 shows the results for the ZB control law in equation (44) for several values of γ. In addition to γ, the control law depends on the parameters p and the gains k_1, k_2, β. The gains k_1 and k_2 were selected as $k_1 = 1$ and $k_2 = 2$. This choice places both poles of the mechanical subsystem (the eigenvalues of the matrix A) at -1. The parameter p in the control law (44) governs the degree of smoothness of the function $u_0(z)^{[2p]}$, hence also of the Lyapunov function itself. The states and control histories become smoother with increasing p. The parameter p can thus be used to control the smoothness and "aggressiveness" of the control law. The value of α in all simulations was chosen as $\alpha = (2p+1)/4$ in order to make the clf homogenous[8] (of degree $2p+1$) with respect to the dilation $\Delta_\lambda(x) = (\lambda^2 x_1, \lambda^2 x_2, \lambda x_3)$. In all simulations, the parameter p was chosen as $p = 1$. From the figures, one concludes that larger values of γ lead to smaller settling times. Similarly, although not explicitly shown, if the gains k_1 and k_2 are selected so that the poles of the matrix A in (23) become more negative, the settling time also decreases. Figure 4 compares zero- and low-bias regulation using (42) for several values of the bias flux. Specifically, simulations for $\Phi_0 = 0,\ 20$ and $100\ \mu$Wb are shown. The gains for the first two cases were chosen as $k_1 = 1$ and $k_2 = 2$, whereas in the third case they were chosen as $k_1 = 1.69$ and $k_2 = 2.6$. This ensures that controllers use approximately the same energy (same area under control voltage signals). The results show that a larger bias results in smaller voltages and shorter settling times, as expected. The effect of the parameters γ, p, k_1, and k_2 in low-bias mode were similar to those for the zero-bias mode and hence the results of these simulations are omitted.

Several simulations with the passivity-based controllers (53), (55), and (57) were also performed. Since the responses

[8] Homogeneity properties of the zero-bias control law (44) are discussed in [18].

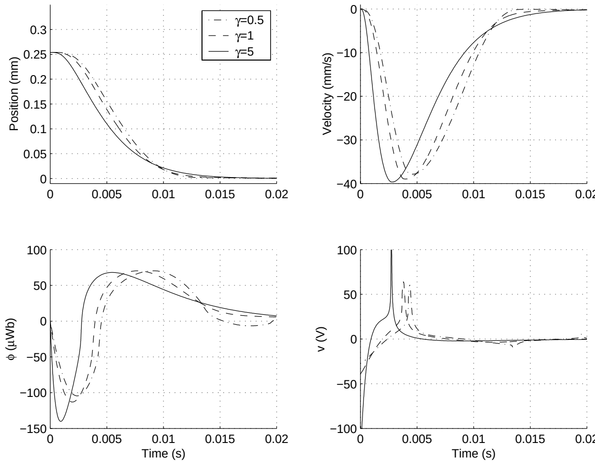

Fig. 3. Zero bias operation with control law (44) for $\beta = 1, p = 1, k_1 = 1, k_2 = 2$, and $\gamma = 0.5, 1, 5$.

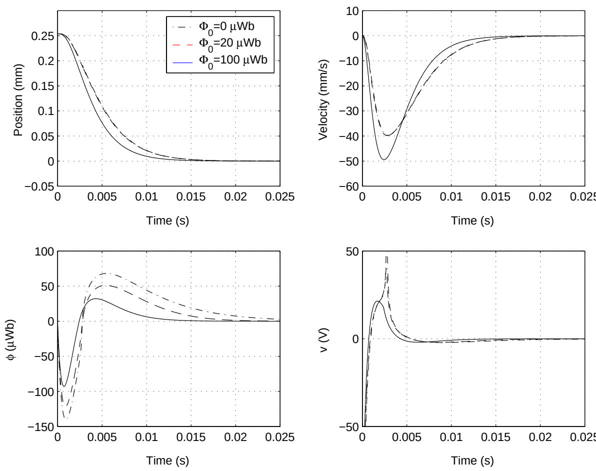

Fig. 4. Zero and Low-bias operation with control law (42) for $\beta = 1, \gamma = 5$ and $p = 1$. Bias flux varied as $\Phi_0 = 0, 20$, and 100 μWb. Gains k_1 and k_2 were chosen to have similar control energy for all cases.

with control laws (53), (55), and (57) were similar, only the results with the control law (53) are shown here for illustration. Figure 5 shows the dependence of the system trajectories and the control input on the control gain γ for ZB operation. The control gains are chosen as $k_1 = 1$ and $k_2 = 2$. As observed in Fig. 5, and similarly to Fig. 3, the settling time decreases as γ increases. This is achieved at the expense of higher voltage commands. Although not explicitly shown, larger values of k_1 result in faster state convergence rates and larger values of k_2 result in more damped responses.

IX. Implementation Issues

In this section we discuss several issues that may arise when implementing the proposed control laws in practice. We also propose some ways to deal with these issues. Although only actual experiments will provide a definite answer to the implementation aspects of the proposed controllers, in lieu of actual experiments herein we present the results of numerical simulations with a high-fidelity AMB model developed by J. Lindlau and C. Knospe [46]. This model includes several

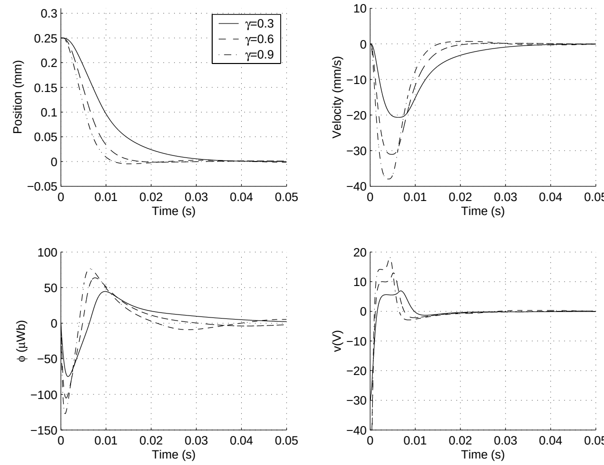

Fig. 5. Zero-bias operation with control law (53) for $k_1 = k_2 = 5$ and $\gamma = 0.3, 0.6, 0.9$.

realistic factors such as coil resistance, voltage and magnetic material saturation, flux leakage, flexibility, etc. Our simulations with this model have corroborated the observations made in the previous section obtained with the ideal AMB model.

A. Implementation of Actual Voltages

When introducing equation (5) it was assumed that the coil resistance is negligible. That is, in Faraday's law

$$N\dot{\Phi}_i = I_i R_i + V_i, \qquad i = 1, 2 \tag{58}$$

the term denoting the voltage drop along the coil $I_i R_i$ was assumed to be small and thus, it could be neglected. Alternatively, a preliminary feedback may be used to cancel this term, using $V_i = V_i' - I_i R_i$, to obtain (5) with $V_i' = V_i$, $i = 1, 2$ instead. The latter approach can be used if a good estimate of the coil resistance R_i is available. Otherwise, robustification of this feedback linearizing control law may be necessary [46]; see also Section IX-D.

Care should also be taken in interpreting the equation $\dot{\phi} = v/N$ between the generalized control flux and the generalized control voltage. It is reminded that the generalized control voltage v is a fictitious control variable used to simplify the control design. The actual voltages applied to each electromagnet V_i should be commanded according to the state-dependent switching (6). As shown in Theorem 1 at steady-state the bearing will operate at a bias level which is determined by the sum of the actual bias Φ_0 and the minimum of the initial values of the control fluxes. Although typically the latter term will be very small (at least when starting the AMB operation from rest) spurious fluxes may still persist. Normally, these remaining spurious control fluxes will help improve the bearing force-slew rate characteristics. In cases where the elimination of these spurious steady-state fluxes is imperative one has several options:

(i) apply any control law to reduce the control flux in at least one of the electromagnets to zero and thus bring the state into the set $\mathcal{S}_0$. For, example, using

$$\begin{aligned} V_1 &= \quad v - \lambda\phi_2, \quad V_2 = -\lambda\phi_2 \quad \text{when} \quad \phi \geq 0 \\ V_2 &= -v - \lambda\phi_1, \quad V_1 = -\lambda\phi_1 \quad \text{when} \quad \phi < 0 \end{aligned}$$

with $\lambda > 0$ instead of (6) one obtains system (11) with $\bar{\Phi}_0(t) := \Phi_0 + \mathrm{e}^{-\lambda t}\min\{\phi_1(0), \phi_2(0)\}$. A deadbeat controller may also be used to drive the trajectories to the set $\mathcal{S}_0$ in finite time.

(ii) Do nothing. In this case, as shown in Theorem 1 the states $(x, \dot{x}) \to 0$ while $\phi_i(t) \to \min\{\phi_1(0), \phi_2(0)\}$. So, stability of the mechanical states of AMB is still ensured, albeit the AMB will operate at a small additional bias. Nonetheless, in practice due to the coil resistance and the resulting dissipation of fluxes even at zero voltage, the AMB states will drift to the set $\mathcal{S}_0$. In that respect, the proposed gcfc switching scheme is forgiving in the presence of nonzero spurious fluxes.

For the numerical simulations of the previous section, the switching strategy (6) was implemented using SIMULINK without any difficulty. Figure 6 shows the control voltages and fluxes for the simulation shown in Fig. 3. It illustrates how the switching of the generalized control input v according to (6) implements the cfc on the total fluxes Φ_2 and Φ_1 (recall that the gcfc strategy (12) and the cfc strategy (13) coincide in this case). In Fig. 6 the flux Φ_1 and the negative of Φ_2 are shown for clarity. For comparison, Fig. 8 shows a simulation with a nonzero bias $\Phi_0 = 20\mu$Wb ($\epsilon = 0.2$) with the high-fidelity model. Figure 8 shows the total fluxes and the corresponding control voltages. It demonstrates how switching of the control input v in accordance with (6) imposes the gcfc constraints on the control fluxes ϕ_1 and ϕ_2. One may verify that both electromagnets are biased, however, only one electromagnet is used at a time to produce a net control force on the rotor.

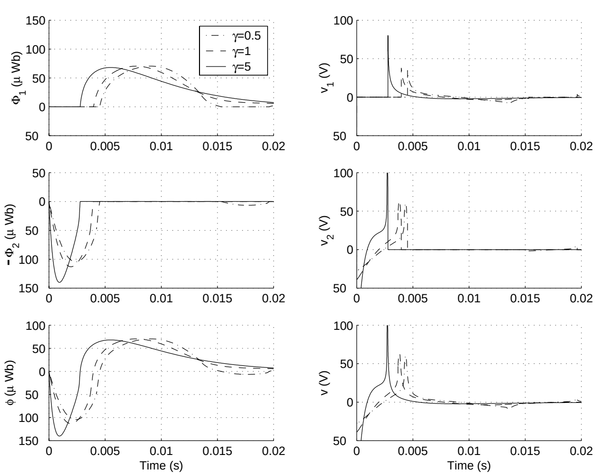

Fig. 6. Zero-bias operation with control law (44) for $p = 1, k_1 = 1, k_2 = 2$, and $\gamma = 5, 10, 15$. Illustration of how the voltage switching rule (6) imposes the cfc constraint on the total fluxes.

B. Implementation of Bias Flux

Using a bias current I_0 has long been a common method for linearizing the AMB equations and achieve acceptable force slew-rate characteristics. While commanding a constant bias current via a transconductance amplifier is straightforward, commanding a constant flux Φ_0 may be not, because the flux depends both on the current as well as the airgap, as follows

$$\Phi = \frac{\mu_0 A_g N I}{2(g_0 \pm x)} \tag{59}$$

With a power amplifier operating in current mode, a position-feedback inner control loop may be used to control the current I in order to regulate the bias flux at Φ_0. With a power amplifier operating in voltage mode a flux-feedback inner loop can be used to regulate the bias flux at Φ_0. Alternatively, one may also use a permanent magnet or a separate coil to generate the bias flux Φ_0. This however, will most likely complicate the overall mechanical design.

In Figures 7 and 8 we have assumed a voltage mode amplifier using a flux-feedback PI inner loop to implement the bias flux. Figure 7, in particular, shows the results of the simulations using the high-fidelity AMB model of [46] (voltage saturation level set to $V_{\rm sat} = 10$ V). In the figures, the dashed line is the ideal model response, i.e., when the plant's flexible modes, coil resistance, flux leakage and voltage saturation are neglected. The solid line is the response of controller (42) with $p = 1$, $\epsilon = 0.2$ ($\Phi_0 = 20\ \mu\mathrm{Wb}$) using the high-fidelity AMB model. The wiggles in the voltage input are due to the flexible modes. Despite the additional effects of the high-fidelity model, the qualitative behavior of the system is similar as in the ideal model case. The discrepancy (mainly delay) in the state trajectories of the actual system in Fig. 7 can be probably traced to the voltage saturation. The effects of voltage saturation during LB operation are dealt with in [47]. From Fig. 8, one also sees that the implementation of the flux bias via a PI flux-feedback inner loop works well. Observe that a bias of $20\mu\mathrm{Wb}$ is quickly established in both electromagnets.

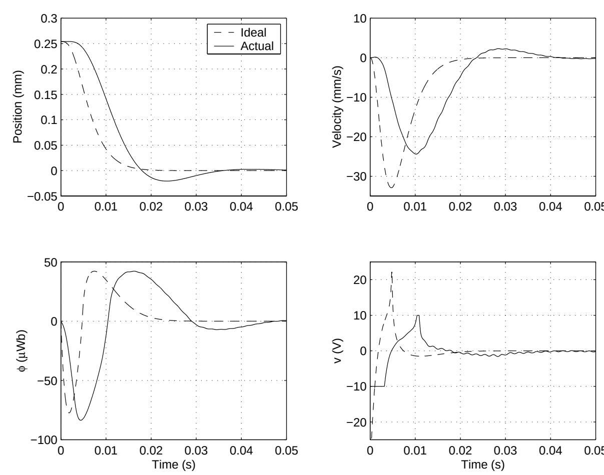

Fig. 7. Comparison of response between ideal and high-fidelity AMB models with control law (42).

C. Flux Feedback

All proposed control laws in this paper use flux measurements for feedback. Although several flux-sensors (Hall

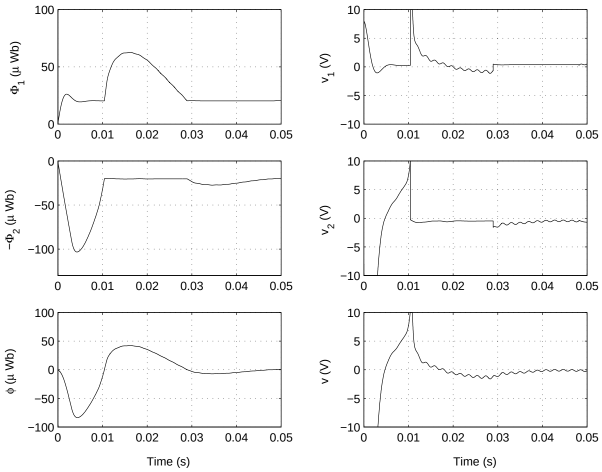

Fig. 8. Illustration of gcfc scheme for the high-fidelity AMB model with control law (42). The total fluxes Φ_1 and Φ_2, the control flux ϕ, and the corresponding control voltages are shown. The bias flux is set to $\Phi_0 = 20\mu$Wb. The signals v_1 and v_2 include the voltages used to set this bias.

sensors) have been developed recently, accurate measurement of the flux still remains a difficult problem [48]. The simplest approach would be to simply use (59) and estimate the flux from current and position measurements. This method was used, for instance in [25]. See, also the discussion in [49], [35], [5]. If no flux sensor is available, a (nonlinear) flux observer can be designed to estimate the flux. For the low-bias case, such an observer has been proposed in [50]. The flux observer in [50] uses x_2 to estimate x_3 in (18b)-(18c). Because the separation principle does not hold for nonlinear systems, the stability of the overall observer/controller design must be explicitly established, however. Such an observer-based design for the low-bias mode has been reported in [47], where voltage saturation is also explicitly taken into account.

D. Robustness to Parameter Uncertainty and Exogenous Disturbances

One of the well-known drawbacks of feedback linearizing controllers is their sensitivity to model uncertainty [51]. The control laws of Sections V and VI deal with an appropriate implementation of the feedback linearizing controller (22) via the integrator (21b). Exact feedback linearization of the mechanical subsystem requires accurate knowledge of the biasing parameter ϵ. In addition, prior to backstepping, these controllers cancel the coil resistance term (see Section IX-A). Thus, it is possible that these control laws may be prone to uncertainties in the AMB model parameters (e.g., coil resistance, bias level, etc.). The passivity-based designs of Section VII are expected to be more robust since they do not depend on the exact cancellation of the nonlinearity at the mechanical subsystem level. Instead, their stabilization properties depend on the monotonicity and oddness of the function f_2 in (18b). Such nonlinearities are considered to be "good" since they satisfy sector conditions in the first/third quadrants [37].

Figure 7 shows that even the control (42) appears to be robust to model uncertainty. In this figure the controller was designed using the ideal plant model (i.e. flexible modes, resistance, flux-leakage, voltage and magnetic material saturation neglected). Nonetheless, it is successfully applied to the high-fidelity model which includes all these effects.

Robustness to parameter uncertainties should be less of an issue for stabilization/regulation problems (as in this paper). On the other hand, model uncertainty and exogenous disturbances could be a major obstacle requiring more close attention in tracking and disturbance rejection problems. For high-speed flywheel applications, for instance, equation (4) will be subject to periodic disturbances due to rotor imbalance or base motion that may cause stability problems. A compromise between low bias (to reduce power losses) and high bias (to achieve sufficient force slew rate) must be achieved. These conflicting performance objectives make disturbance rejection in low- and/or zero-bias mode a challenging problem, appropriate for future investigation.

X. CONCLUSIONS

Low loss operation is important in several AMB applications, such as in high-speed energy flywheel systems, artificial heart pump impellers, etc. Since eddy current and ohmic losses are proportional to the flux, low-bias (LB) and zero-bias (ZB) control schemes for AMBs are advantageous for low-loss operation of AMBs. The main obstacle in deriving LB/ZB control algorithms for an AMB is the nonlinearity of the associated mathematical model. In this paper we propose several schemes for low-bias and zero-bias control of active magnetic bearings. Using a flux-based, voltage-controlled AMB model, we propose a series of new control laws borrowing from a variety of tools available in modern nonlinear control theory: control Lyapunov functions, integrator backstepping, homogeneity and passivity. For the zero-bias case, in particular, our control designs emphasize the mitigation of the control singularity encountered in typical ZB designs. Comparison of simulation results between an ideal and a high-fidelity AMB model were very promising. Future work will concentrate on the experimental testing of the proposed control laws on an actual active magnetic bearing.

ACKNOWLEDGMENT

The authors would like to thank Prof. Eric Maslen, Prof. Carl Knospe and Prof. Marcio de Queiroz for their insightful comments during the preparation of this manuscript. They would also like to thank Prof. C. Knospe for providing the SIMULINK model of the high-fidelity AMB model.

APPENDIX

Let the function $x^{[q]} = \mathrm{sgn}(x)x^q$ where q is a positive integer. It is easy to verify that the above function has the following properties.

1) $x^{[q]}x^{[p]} = x^{p+q}$ and $x^{[q]}x^p = x^{[p+q]}$
2) $\frac{x^{[p]}}{x^{[q]}} = x^{p-q}$ and $\frac{x^{[p]}}{x^q} = x^{[p-q]}$
3) $\frac{\mathrm{d}x^{[p]}}{\mathrm{d}x} = p\,x^{[p-1]}$ and $\int x^{[p]}\,\mathrm{d}x = \frac{x^{[p+1]}}{p+1}$
4) If a scalar function f is homogeneous of degree p then $f^{[q]}$ is homogeneous of degree pq.

5) $x^{[q]} \in \mathcal{C}^0$ for $q > 0$.
6) $x^{[q]} \in \mathcal{C}^1$ for $q \geq 2$.
7) If q is an odd integer, then $x^{[q]}$ is an even function.
8) If q is an even integer, then $x^{[q]}$ is an odd function.

References

[1] M. D. Anderson and S. C. Dodd, "Battery energy storage technologies," *Proceedings of the IEEE*, vol. 81, no. 3, pp. 475–479, 1993.

[2] R. F. Post, T. K. Fowler, and S. F. Post, "A high-efficiency electromechanical battery," *Proceedings of the IEEE*, vol. 81, no. 3, pp. 470–474, 1993.

[3] Anonymous, "The flywheel revolution," *Electrical Review*, vol. 230, no. 13, pp. 18–20, 1995.

[4] C. Knospe, "The nonlinear control benchmark experiment," in *Proceedings of the American Control Conference*, pp. 2134–2138, 2000. Chicago, IL.

[5] M. Baloh, G. Tao, and P. Allaire, "Modeling and control of a magnetic bearing actuated beam," in *Proceedings of the American Control Conference*, pp. 1602–1606, 2000. Chicago, IL.

[6] J. Ghosh, D. Mukherjee, B. M., and B. Paden, "Nonlinear control of a benchmark beam balance experiment using variable hyperbolic bias," in *Proceedings of the American Control Conference*, pp. 2149–2153, 2000. Chicago, IL.

[7] L. Li and J. Mao, "Feedback linearization of magnetic bearing actuators for a uniform upper bound of force slew rate," *IEE Proc.-Electr. Power Appl.*, vol. 146, no. 4, pp. 378–382, 1999.

[8] K. Bornstein, "Dynamic capabilities of active magnetic bearings," *ASME Journal on Tribology*, vol. 113, pp. 598–603, 1991.

[9] E. Maslen, P. Hermann, and M. Scott, "Practical limits to the performance of magnetic bearings: Peak force, slew rate and displacement sensitivity," *ASME Journal on Tribology*, vol. 111, pp. 331–336, 1989.

[10] A. Charara, J. De Miras, and B. Caron, "Nonlinear control of a magnetic levitation system without premagetization," *IEEE Transactions on Control Systems Technology*, vol. 4, no. 5, pp. 513–523, 1996.

[11] J. Lottin, P. Mouille, and J. C. Ponsart, "Nonlinear control of active magnetic bearings," in *Proceedings of the 4th International Symposium on Magnetic Bearings*, pp. 101–106, 1994. ETH, Zurich.

[12] A. Charara and B. Caron, "Magnetic bearing: Comparison between linear and nonlinear functioning," in *Proceedings of the 3rd International Symposium on Magnetic Bearings*, pp. 451–463, 1992.

[13] R. D. Smith and W. F. Weldon, "Nonlinear control of a rigid rotor magnetic bearing system: Modeling and simulation with full state feedback," *IEEE Transactions on Magnetics*, vol. 31, pp. 973–980, Mar. 1995.

[14] S. Mittal and C. Menq, "Precision motion control of a magnetic suspension actuator using a robust nonlinear compensation scheme," *IEEE/ASME Transactions on Mechatronics*, vol. 2, pp. 268–280, Dec. 1997.

[15] M. Torries, H. Sira-Ramirez, and G. Escobar, "Sliding mode nonlinear control of magnetic bearings," in *Proceedings of the IEEE International Conference on Control Applications*, pp. 743–748, 1999.

[16] D. Cho, Y. Kato, and D. Spilman, "Sliding mode and classical controllers in magnetic levitation systems," *IEEE Control Systems Magazine*, vol. 14, no. 2, pp. 4–12, 1994.

[17] J. Lévine, J. Lottin, and J. C. Ponstart, "A nonlinear approach to the control of magnetic bearings," *IEEE Transactions on Control Systems Technology*, vol. 4, pp. 524–544, Sept. 1996.

[18] P. Tsiotras, B. C. Wilson, and R. O. Bartlett, "Control of a zero-bias magnetic bearing using control Lyapunov functions," in *Proceedings of the 39th IEEE Conference on Decision and Control*, pp. 4048–4053, 2000. Sydney, Australia.

[19] M. S. de Queiroz and D. M. Dawson, "Nonlinear control of active magnetic bearings: A backstepping approach," *IEEE Transactions on Control Systems Technology*, vol. 4, no. 5, pp. 545–552, 1996.

[20] M. S. de Queiroz, D. M. Dawson, and H. Canbolat, "A backstepping-type controller for a 6-dof active magnetic bearing system," in *Proceedings of the 35th IEEE Conference on Decision and Control*, pp. 3370–3375, 1996. Kobe, Japan.

[21] M. S. de Queiroz, D. M. Dawson, and A. Suri, "Nonlinear control of a large gap 2-dof magnetic bearing system based on a coupled force model," in *Proceedings of the American Control Conference*, pp. 2165–2169, 1997. Albuquerque, NM.

[22] P. Tsiotras and E. Velenis, "Low-bias control of AMB's subject to saturation constraints," in *IEEE International Conference on Control Applications*, pp. 138–143, 2000. Ancorage, AK.

[23] C. Knospe and C. Yang, "Gain-scheduled control of a magnetic bearing with low bias flux," in *Proceedings of the 36th Conference on Decision and Control*, pp. 418–423, 1997. San Diego, CA.

[24] C. Knospe, "The nonlinear control benchmark experiment," in *Proceedings of the American Control Conference*, pp. 2134–2138, 2000. Chicago, IL.

[25] Z. Lin and C. Knospe, "A saturated high gain control for a benchmark experiment," in *Proceedings of the American Control Conference*, pp. 2644–2648, 2000. Chicago, IL.

[26] H. Rodriguez, R. Ortega, and I. Mareels, "A novel passivity-based controller for an active magnetic bearing benchmark experiment," in *Proceedings of the American Control Conference*, pp. 2144–2148, 2000. Chicago, IL.

[27] B. T. Costic, M. S. de Queiroz, and D. M. Dawson, "A new learning control approach to the active magnetic bearing benchmark system," in *Proceedings of the American Control Conference*, pp. 2639–2643, 2000. Chicago, IL.

[28] N. Motee, M. S. de Queiroz, Y. Fang, and D. M. Dawson, "Active magnetic bearing control with zero steady-state power loss," in *Proceedings of the American Control Conference*, pp. 827–832, 2002. Anchorage, AK.

[29] L. Praly, B. d'Andréa-Novel, and J. M. Coron, "Lyapunov design of stabilizing controllers for cascaded systems," *IEEE Transactions on Automatic Control*, vol. 36, no. 10, pp. 1177–1181, 1991.

[30] N. N. Rao, *Elements of Engineering Electromagnetics*. Englewood Cliffs, NJ: Prentice Hall, 4th ed., 1994.

[31] V. Chellaboina and W. M. Haddad, "A unification between partial stability and stability theory for time-varying systems," *IEEE Control Systems Magazine*, vol. 22, no. 6, pp. 66–75, 2002.

[32] V. I. Vorotnikov, *Partial Stability and Control*. Boston, MA: Birkhäuser, 1998.

[33] C. Yang, C. Knospe, and P. Tsiotras, "Optimal control of a magnetic bearing without bias and saturating voltages," *Optimal Control Applications and Methods*, vol. 19, pp. 227–246, 1998.

[34] P. Allaire, M. Kasarda, and L. K. Fujita, "Rotor power losses in planar radial magnetic bearings - effects of number of stator poles, air gap thickness, and magnetic flux density," in *Proceedings of the 1998 International Gas Turbine and Aeroengine Congress and Exhibition*, 1998. Stockholm, Sweden.

[35] L. Li, "Linearizing magnetic bearing actuators by constant current sum, constant voltage sum, and constant flux sum," *IEEE Transactions on Magnetics*, vol. 35, no. 1, pp. 528–535, 1999.

[36] M. Krstić, I. Kanellakopoulos, and P. Kokotović, *Nonlinear and Adaptive Control Design*. New York, NY: Wiley-Interscience, 1995.

[37] R. Sepulchre, M. Janković, and P. Kokotović, *Constructive Nonlinear Control*. London, England: Springer-Verlag, 1997.

[38] E. D. Sontag, "A universal consruction of Artstein's theorem on nonlinear stabilization," *Systems and Control Letters*, vol. 13, pp. 117–123, 1989.

[39] H. Hermes, "Nilpotent and high order approximations of vector field systems," *SIAM Review*, vol. 33, pp. 238–264, 1991.

[40] R. T. M'Closkey and R. M. Murray, "Exponential stabilization of driftless nonlinear control systems using homogeneous feedback," *IEEE Transactions on Automatic Control*, vol. 42, no. 5, pp. 614–628, 1997.

[41] C. A. Desoer and M. Vidyasagar, *Feedback Systems: Input-Output Properties*. New York: Academic Press, 1975.

[42] R. Ortega, A. Loría, P. J. Nicklasson, and H. Sira-Ramírez, *Passivity Based Control of Euler-Lagrange Systems: Mechanical, Electrical and Electromechanical Applications*. London, England: Springer-Verlag, 1998.

[43] R. G. Bartle, *The Elements of Real Analysis*. New York: John Wiley & Sons, 1976.

[44] H. K. Khalil, *Nonlinear Systems*. New Jersey: Prentice Hall, 2nd ed., 1996.

[45] A. Teel and M. Arcak, August 2000. Private Communication.

[46] J. D. Lindlau and C. Knospe, "Feedback linearization of an active magnetic bearing with voltage control," *IEEE Transactions on Control Systems Technology*, 2001. to appear.

[47] P. Tsiotras and M. Arcak, "Low-bias control of AMB subject to voltage saturation: State-feedback and observer designs," in *Proceedings, 41st IEEE Conference on Decision and Control*, pp. 2474–2479, 2002. Las Vegas, NV.

[48] F. Keith, *Implicit Flux Feedback Control for Magnetic Bearings*. PhD thesis, University of Virginia, Charlottesville, Virginia, 1993.

[49] E. Maslen, "Magnetic Bearings." Graduate Seminar Notes, Dept. of Mechanical and Aerospace Engineering, University of Virginia, June 2000.

[50] M. Arcak and P. Kokotović, "Observer-based control of systems with slope-restricted nonlinearities," *IEEE Transactions on Automatic Control*, vol. 46, 2001.

[51] D. L. Trumper, "Linearizing control of magnetic suspension systems," *IEEE Transactions on Control Systems Technology*, vol. 5, no. 4, pp. 427–438, 1997.

Panagiotis Tsiotras is Associate Professor in the School of Aerospace Engineering at the Georgia Institute of Technology. From 1994-1998 he was Assistant Professor with the Department of Mechanical and Aerospace Engineering at the University of Virginia. Professor Tsiotras received his Ph.D. degree in Aeronautics and Astronautics from Purdue University in 1993, his M.Sc. degree in Aerospace Engineering from Virginia Tech in 1987, and his Engineering Diploma in Mechanical Engineering from the National Technical University of Athens, Greece in 1986. He also holds an M.Sc. degree in Mathematics from Purdue University (1992). Professor Tsiotras is a recipient of the NSF CAREER Award (1996). He is Associate Editor of the *AIAA Journal of Guidance, Control, and Dynamics* and the *IEEE Control Systems Magazine*. His research interests include dynamics and control of nonlinear systems, and optimal and robust control with applications to mechanical and aerospace systems.

Brian C. Wilson was born in Buffalo, NY in 1973. He received his BS in Electrical Engineering from SUNY Buffalo in 1996 and a Masters of Electrical Engineering from the Georgia Institute of Technology in 1998. In the summer of 2001, he participated in the Air Force Research Labs Space Scholars Program at Kirtland AFB, NM. He is currently a Ph.D. candidate in the School of Electrical Engineering at Georgia Tech. His current research interests include analytical dynamics, nonlinear control theory, electromechanical machines, active magnetic bearings, and electronic instrumentation.